Rare Metal Materials and Engineering
Volume 49, Issue 1, January 2020
Available online at www.rmme.ac.cn

Science Press

Cite this article as: Rare Metal Materials and Engineering, 2020, 49(1): 0001-0009.

ARTICLE

Effect of Nd on Microstructure and Mechanical Properties of Mg-Al-Ca Alloy

Yang Donghu[1], Chen Xianhua[2,3], Xu Xiaoyang[2], Zhao Chaoyue[2,3]

[1] Beijing Institute of Technology, Beijing 100081, China; [2] College of Materials Science and Engineering, Chongqing University, Chongqing 400044, China; [3] National Engineering Research Center for Magnesium Alloys, Chongqing University, Chongqing 400044, China

Abstract: The microstructures and precipitated phases of as-extruded Mg-Al-Ca-*x*Nd alloys with *x*=0 wt%~1.76 wt% Nd were studied by OM, SEM and XRD. The mechanical properties of the alloys at room temperature and high temperature were also tested. Results show that the addition of Nd results in the formation of Al_2Nd and $Al_{11}Nd_3$ phases in the matrix and the grain refinement of Mg-Al-Ca alloy, and the amount of Al_2Nd and $Al_{11}Nd_3$ phases increases with the increase of Nd addition. The average grain size of these alloys changes from 4.80 μm (without Nd) to 2.39 μm (with 1.76 wt% Nd added). The mechanical properties at room temperature are improved due to the precipitation of the second phases and grain refinement. With increment of Nd, the tensile strength increases from 267 MPa to 304 MPa, the yield strength increases from 144 MPa to 203 MPa and the elongation decreases from 20.0% to 16.9% at room temperature. At 150 ℃, the tensile strength increases from 192 MPa to 229 MPa, the yield strength increases from 140 MPa to 159 MPa and the elongation decreases from 48.6% to 29.3% with increasing the Nd content.

Key words: Mg-Al-Ca-Nd alloys; as-extruded; microstructure; mechanical properties

During the last few decades, the world has paid considerable attention to magnesium and its alloys, which have gained more and more extended applications in the 3C applications and aerospace industries by virtue of combination of low density, superior damping capacity, high specific strength, and high specific stiffness[1-4]. However, the commercialization of magnesium alloys is hindered by their low strength and poor ductility due to their hexagonal close-packed crystal structure[5-8]. Among the various Mg-based alloy systems that have been well developed, Mg-Al alloy systems are the most widely used in engineering components because of their good cast ability, low cost, and moderate strength at room temperature[9,10]. However, their wider application has been restricted by their low creep resistance above 120 ℃, which is caused by the formation of discontinuous precipitation of $Mg_{17}Al_{12}$ phase with a relatively low eutectic temperature of 437 ℃ [11]. Previous studies proved that mechanical properties of magnesium alloys at elevated temperatures are strongly related to the thermally stable secondary phases they contain. Conventional alloying method is regarded as an effective way for improving the mechanical performance at both RT and elevated temperature. And creep resistance of Mg alloys has been successfully improved by element alloying, since second phases are more thermally stable[12, 13].

It is well known that addition of calcium to magnesium is effective in preventing high-temperature oxidation and improving the creep resistances. The calcium addition is also effective in grain refinement of magnesium castings[14,15], due to hard and thermally stable Al_2Ca or $(Al, Mg)_2Ca$ phase that prefers to exist at grain boundaries during solidification of Mg-Al-Ca alloys, and can provide recrystallization nucleation sites, leading to effective grain refinement during plastic deformation[16,17]. Alloying Mg with rare earth (RE) elements has received considerable attention, which can attain the desired strength and ductility of Mg

Received date: January 17, 2019
Corresponding author: Chen Xianhua, Ph. D., Professor, College of Materials Science and Engineering, Chongqing University, Chongqing 400044, P. R. China, Tel: 0086-23-65102633, E-mail: xhchen@cqu.edu.cn

alloys. A great number of researches [18-21] have indicated that the addition of Nd to Mg-Al alloys can form high-melting point Al-Nd secondary phase such as $Al_{11}Nd_3$, Al_2Nd, and Al_3Nd, as well as induce other positive effect like grain refinement. All of these combine to improve the high temperature strength.

Previous study[22] has revealed that an improvement in the tensile properties of ECAPed Mg-15Al (wt%) alloy can be achieved by adding 1.5 wt% Nd, with the yield strength (YS), ultimate tensile strength (UTS) and elongation being increased by 54.2%, 24.4% and 21% at RT, and 19.4%, 20.8% and 17.9% at 150 ℃, respectively. Such result indicates the huge potential of Mg-Al-Nd magnesium alloys. However, there are few studies reported on the exact effect of content variation of the rare earth element Nd on the microstructure and mechanical performance of Mg-3Al-0.5Ca-Nd in as-cast and extruded conditions. The aim of this study is to elucidate the effects of Nd addition on the microstructure and mechanical properties of indirectly extruded Mg-Al-Ca-Nd alloy, and to clarify their relationship.

1 Experiment

Four alloys were prepared and the nominal chemical composition of the alloys is Mg-3Al-0.5Ca (alloy I), Mg-3Al-0.5Ca-0.5Nd (alloy II), Mg-3Al-0.5Ca-1Nd (alloy III), Mg-3Al-0.5Ca-2Nd (alloy IV). The alloy ingots with nominal composition of Mg-Al-Ca-*x*Nd were produced using commercially high purity Mg (99.98 wt%), Al (99.98 wt%), and master alloys of Mg-30Ca (wt%) and Mg-25Nd (wt%).

The alloys were melted in an electric-resistant furnace under an inert atmosphere of CO_2 and SF_6 mixture. When the temperature reached 750 ℃, molten alloys were stirred for 8 min and subsequently held for 30 min. Then they were poured into a steel mold pre-heated to 200 ℃, and the cylindrical ingots with a diameter of 90 mm were made. Specimens were cut from the ingot by an electric spark linear cutting machine. The amounts of Nd added to the four alloys are 0 wt%, 0.5 wt%, 1 wt% and 2 wt%.

The actual chemical composition of these alloys was determined by an inductively coupled plasma analyzer (ICP), as listed in Table 1. The hot extrusion was carried out on the received ingots at the temperature of 350 ℃ with an extrusion ratio of 25:1 to obtain as-extruded bars. Before extrusion, the cast ingots were preheated at 450 ℃ for 12 h.

The constituent phases of as-cast alloys were identified by X-ray diffraction (XRD, Rigaku D/MAX-2500PC) using a copper target with a scanning angle of 10°~90° and a scanning speed of 2°/min. Microstructure observations were conducted using a scanning electron microscope (SEM, TESCAN VEGA II LUM) with energy dispersive spectrum (EDS) operated at 20 kV. For SEM observation, the polished specimens were etched with a mixture of 0.8 g picric acid, 10 mL ethanol, 2 mL acetic acid and 2 mL water. The grain size was measured by Image-pro-plus.

Tensile testing was performed using a CMT-5105 material testing machine with a strain rate of 1×10^{-3} s^{-1} at room temperature and 150 ℃. The extruded bars were cut into rectangular tensile specimens with a gage length of 25 mm and a cross-sectional area of 2 mm×5 mm by an electrical sparking wire cutting machine. Each test condition was repeated at least three times for repeatability and accuracy. Tensile direction was parallel to extrusion direction. The heating-plus-holding time was 10 min for equilibrating the temperature before tensile test at elevated temperatures. The fracture surfaces of the tensile specimens were also analyzed by OM and SEM.

2 Results and Discussion

2.1 Microstructure and texture of as-cast and extruded alloys

XRD patterns of the as-cast alloys are illustrated in Fig.1. It reveals that the quantity and composition of the second phases change with the increase of Nd content. The profile for Nd-free AX30 alloy includes peaks from α-Mg, $Mg_{17}Al_{12}$ and Al_2Ca phases. Generally, Al has two forms in AX30 based alloys: dissolving in the α-Mg matrix and reacting with Mg to form $Mg_{17}Al_{12}$ compounds. But this situation changed when Nd was added into the Mg-Al base alloys, because the precipitation of Al-Nd phases would consume Al elements in AX30 alloy. As shown Fig.1, peaks of $Mg_{17}Al_{12}$ phase are suppressed with the Nd addition, and additional peaks of $Al_{11}Nd_3$ and Al_2Nd phase emerge in the alloy II~IV.

Fig.2 presents SEM images of the as-cast Mg-Al-Ca-*x*Nd alloys. It can be seen that the Nd-free alloy is composed of three types of phases: gray α-Mg, rod-shaped phase, and island-shaped phase. With addition of 1.11 wt% Nd, some polygonal precipitates and acicular precipitates appear in the alloy with 1.11wt% Nd. The volume fraction of acicular precipitate increases with increasing the Nd content, while island-shaped phase decreases and even disappears. EDS analysis presented in Table 2 shows chemical composition of four representative points marked A~D in Fig.2, in which A is labeled for the island-shaped phase, B for the rod-shaped phase, C for the polygonal phase, and D for the acicular phase. EDS analysis result suggests that the island-shaped

Table 1 Chemical composition of as-cast Mg-Al-Ca-Nd alloys (wt%)

Alloy	Al	Ca	Nd	Mg
I	2.90	0.42	0	Bal.
II	2.85	0.44	0.62	Bal.
III	2.79	0.39	1.11	Bal.
IV	2.80	0.37	1.76	Bal.

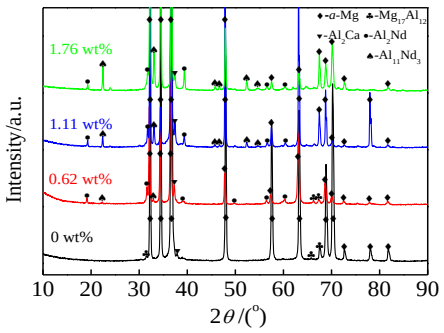

Fig.1 XRD patterns of the as-cast Mg-Al-Ca-Nd alloys with different Nd contents

phase (point A) is rich in Al, considered as $Mg_{17}Al_{12}$ according to XRD result. The bright phases formed as rod-like (point B) phase is rich in Al and Ca, which is determined as Al_2Ca based on the Al:Ca atom ratio close to 2:1 and XRD result. The atomic ratio of Al:Nd for the polygon particles with size of 3~4 μm labeled as C is 2.09:1, very close to the stoichiometric ratio 2:1 for Al_2Nd phase. While for the large amount of aciculate phases with width of about 200 nm and length of about several microns labeled as D, EDS result reveals that Al:Nd ratio is 3.71:1, close to 11:3 for the chemical formulas $Al_{11}Nd_3$ phase. Fig.2 reveals that the volume fraction of $Al_{11}Nd_3$ phase increases with increasing the Nd content, while the $Mg_{17}Al_{12}$ phase decreases, and even disappears. This is also confirmed by the XRD analysis (Fig.1).

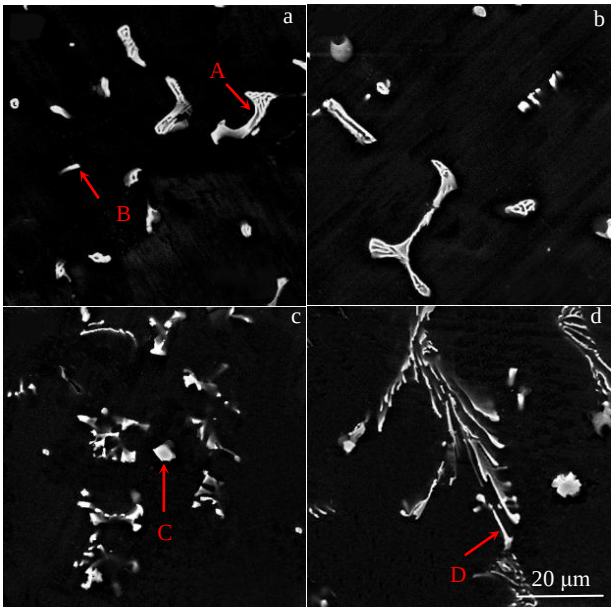

Fig.2 SEM micrographs of the as-cast Mg-Al-Ca-*x*Nd alloys: (a) 0 wt%, (b) 0.62 wt%, (c) 1.11 wt%, and (d) 1.76 wt%

Table 2 EDS results of points marked as A~D in Fig.2

Point	Mg		Al		Ca		Nd		Phase
	at%	wt%	at%	wt%	at%	wt%	at%	wt%	
A	65.31	70.29	34.69	29.71	-	-	-	-	$Mg_{17}Al_{12}$
B	73.52	68.15	17.28	17.78	9.20	14.06	-	-	Al_2Ca
C	10.93	8.72	60.25	53.36	-	-	28.82	37.92	Al_2Nd
D	68.44	50.42	24.87	20.34	-	-	6.69	29.24	$Al_{11}Nd_3$

Fig.3 shows DSC results of as-cast Mg-Al-Ca-*x*Nd alloys during the heating process. For the four alloys, there is a first endothermic peak at the temperature of about 440 ℃, which can be considered as the melting temperature of $Mg_{17}Al_{12}$ phase ($T_m(Mg_{17}Al_{12})$=437 ℃). However, the second endothermic peak appears at about 635 ℃, which corresponds to the melting temperature of *α*-Mg matrix. The volume fraction of Al_2Ca phase in the matrix is too low, so it is hard to detect its endothermic peak, while no endothermic peaks of $Al_{11}Nd_3$ and Al_2Nd phases can be observed due to their high melting points ($T_m(Al_2Nd)$=1205 ℃ and $T_m(Al_{11}Nd_3)$=1235 ℃).

Adding Nd into Mg-3Al-0.5Ca alloy leads to the suppression of $Mg_{17}Al_{12}$ phase formation in the range of tested Nd content, and Nd is combined with Al to form Al-Nd phases. The possibility to form metallic compounds is relative to the two elements' electronegativity difference, which means

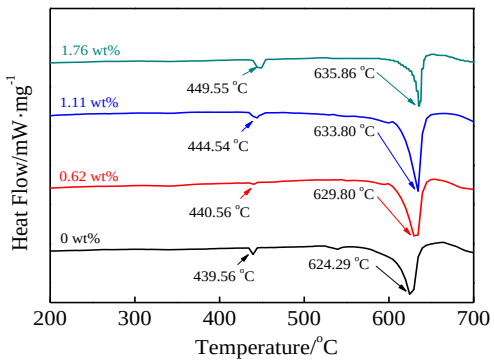

Fig.3 DSC curves of as-cast Mg-Al-Ca-*x*Nd alloys

that the larger the differences between two elements, the stronger the bonding force between them, and the easier the formation of a metallic compound[23,24]. The electronegativities of Mg, Al and Nd are 1.31, 1.61 and 1.14, respectively [25]. It is obvious that the difference in electronegativity between Nd and Al is larger than that between Nd and Mg. In addition, the formation temperature of Al-Nd phase (T_m(Al_2Nd)=1205 ℃ and T_m($Al_{11}Nd_3$)=1235 ℃) is much higher than that of $Mg_{17}Al_{12}$ phase (T_m($Mg_{17}Al_{12}$)=437 ℃), which means that the formation of Al-Nd phase precedes that of $Mg_{17}Al_{12}$ phase.

Therefore, when Nd element is added, Nd atom preferentially reacts with Al to form Al-Nd compound rather than the Mg-Nd compound during solidification. Similar results have been reported that Al_2Nd particles are formed as pro-eutectic phases and $Al_{11}Nd_3$ compound is regarded as the product of peritectic reaction [26]:

$$3\,Al_2Nd+L\rightarrow Al_{11}Nd_3 \quad (1)$$

Fig.4 shows the OM images of the extruded Mg-Al-Ca-*x*Nd alloys. The extruded alloys exhibit uniform and equiaxed grains, indicating that a complete dynamic recrystallization process happens during extrusion. It also reveals that the grain sizes of these alloys decrease remarkably with increasing the Nd content. Based on statistical measurements, the average grain sizes were measured to be 4.80, 4.13, 2.70 and 2.39 μm for the alloys with 0 wt%, 0.66 wt%, 1.11 wt% and 1.76 wt% Nd, respectively. Furthermore, when the content of Nd increased from 1.11 wt% to 1.76 wt%, more black eutectic or intermetallic phases in the vicinity of grain boundaries appeared.

The grain refinement might be attributed to the enrichment of Nd, which promoted nucleation in the melt, elevated the formation temperature of Al-Nd-rich intermetallic compounds, increased the impediment effect of constitutional undercooling in a diffusion layer ahead of the advancing solid/liquid interface and lowered the extent of the eutectic reaction, all of which are important reasons for the refined alloy in this study.

Typical SEM images of extruded Mg-Al-Ca-*x*Nd alloys are illustrated in Fig.5. Evidently, in these alloys, broken particles are dispersed in the α-Mg matrix after hot extrusion. Meanwhile, the amount of particles increases with Nd addition. For these alloys, hot extrusion make secondary phase to be pocketed away and destroyed them into smaller particles.

The granular phases in alloy I as well as the rod-shaped and polygon particles in alloy IV were determined as Al_2Ca, $Al_{11}Nd_3$ and Al_2Nd by EDS analysis, respectively. After the homogenization heat treatment at 450 ℃, $Mg_{17}Al_{12}$ was dissolved in the α-Mg matrix and cannot be observed by XRD

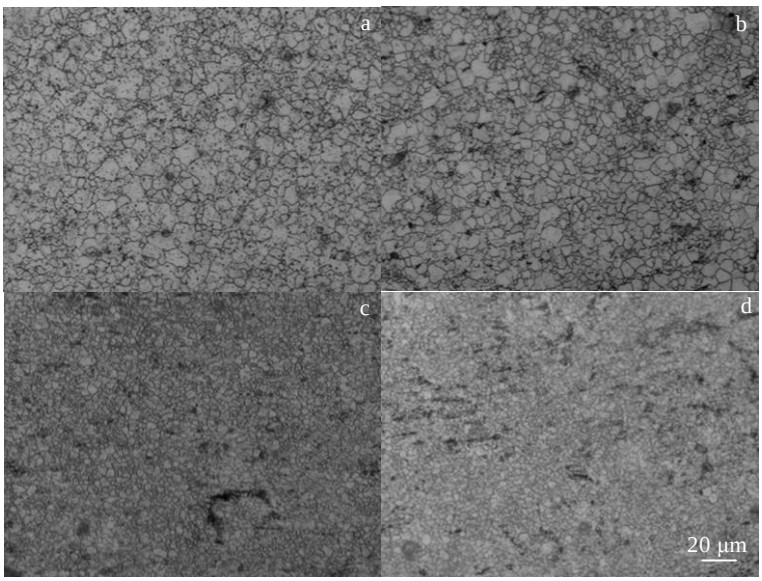

Fig.4 OM images of the extruded Mg-Al-Ca-*x*Nd alloys: (a) 0 wt%, (b) 0.62 wt%, (c) 1.11 wt%, and (d) 1.76 wt%

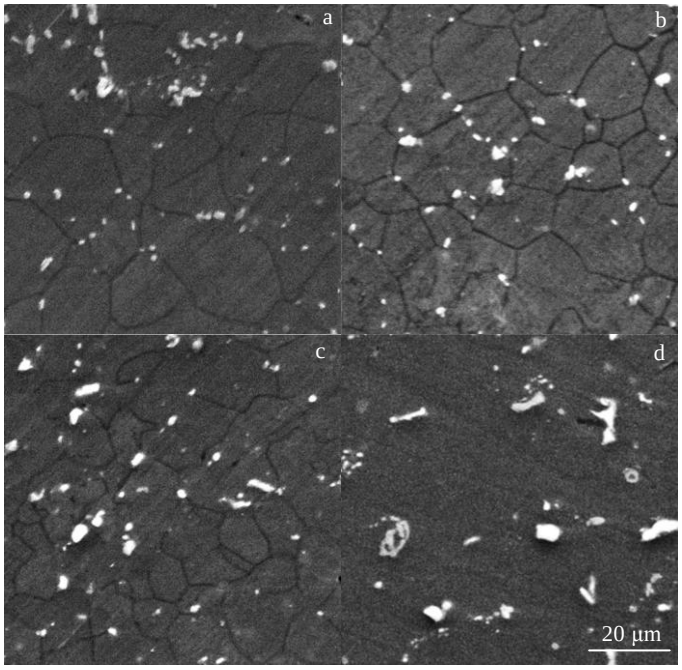

Fig.5 SEM images of extruded Mg-Al-Ca-*x*Nd alloys: (a) 0 wt%, (b) 0.62 wt%, (c) 1.11 wt%, and (d) 1.76 wt%

and SEM-EDS. Fig.6 shows EDS maps of the extruded alloy IV. It was found that Al exists in both second phase and matrix. However, it is preferred to form second phases with Nd.

2.2 Mechanical properties of extruded alloys at RT and elevated temperatures

Mechanical properties of the extruded alloy were tested at room temperature (RT) and 150 ℃ along the loading directions of ED. Fig.7 illustrates the stress-strain curves of the extruded alloy at RT and 150 ℃. Ultimate tensile strength (UTS), yield strength (YS) and elongation are listed in Table 3.

Nd-free alloy I exhibits a yield strength of 144 MPa and an ultimate tensile strength of 267 MPa at RT. The small amount of Nd addition (0.62 wt%) considerably improves the strengths of the alloy II: YS of 176 MPa, UTS of 281 MPa, and elongation decreases slightly. After further adding Nd, yield strength and ultimate tensile strength significantly increase, but the ductility performance substantially deteriorates. This enhancement of strength due to Nd addition is generally influenced by contributions from grain refinement and precipitation strengthening.

Firstly, the refined grains and homogeneous microstructure after adding Nd are helpful for the increment in yield strength and ultimate tensile strength of the alloys. It is known that grain size and yield strength are inversely related, as demonstrated by the Hall-Petch equation [27]:

$$\sigma=\sigma_0+kd^{-1/2} \quad (2)$$

in which σ_0 is frictional stress, k is the Hall-Petch coefficient, and d is grain size. If assuming that all the extruded alloys in this study have an identical frictional stress and Hall-Petch coefficient, the increase in yield stress due to grain refinement by Nd addition can be expressed as follows[28]:

$$\Delta\ \sigma_{gb}=k(d_{\text{Mg-Al-Ca-}x\text{Nd}}^{-1/2}-d_{\text{Mg-Al-Ca}}^{-1/2}) \quad (3)$$

From the k value of 170 MPa·μm$^{-1/2}$ for the present extruded alloy, and the measured average grain sizes of these four extruded a1loys of 4.80, 4.13, 2.70, and 2.39 μm, the increment of yield stress due to grain refinement was calculated as 6, 25.8, and 28 MPa for the alloys II~IV, respectively.

Secondly, the analysis of precipitate strengthening, microstructure and mechanical properties reveals that the fraction of fine particles precipitated from a supersaturated solid solution during extrusion increases with increasing the Nd addition. These hard $Al_{11}Nd_3$ and Al_2Nd particles dispersed in a soft Mg matrix can provide an effective barrier to dislocation movement during deformation, which increases the strength of the material[20, 22, 29, 30].

However, although the maximum solubility of Nd in α-Mg matrix is 3.6%[31,32], contribution from solution strengthening is restricted in Mg-Al-Ca alloy. Nd element tends to form second phases with Al element, so there is little Nd dissolved in the Mg matrix and the solution strengthening is negligible[32, 33].

In the present alloys, alloy I exhibits a relatively good elongation of 20%. On the contrary, as the addition of Nd increases, the elongation gradually decreases in spite of the

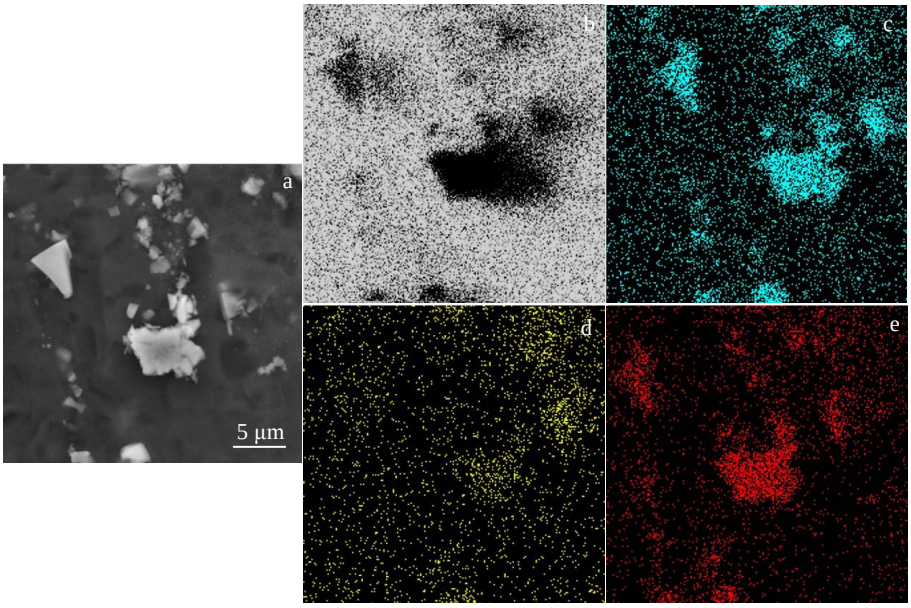

Fig.6 SEM image (a) of extruded alloy IV and corresponding EDS mapping of Mg (b), Al (c), Ca (d) and Nd (e)

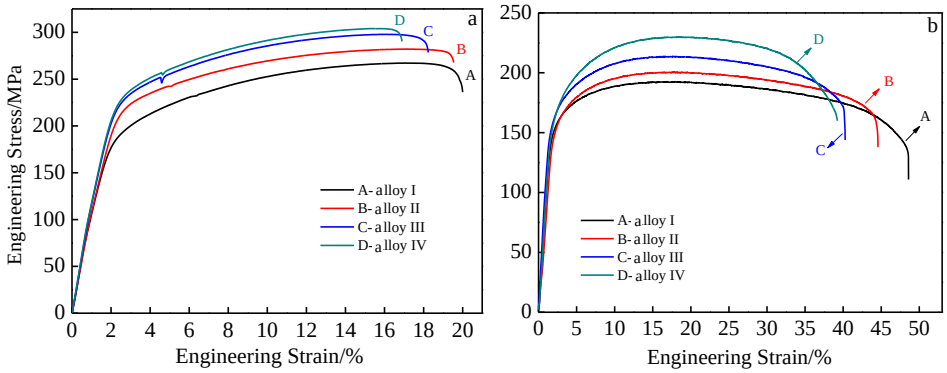

Fig.7 Typical tensile engineering stress-strain curves of the extruded Mg-Al-Ca-*x*Nd samples: (a) RT and (b) 150 ℃

decrease in grain size, which benefits the ductility. This result is induced by the large amount of hard $Al_{11}Nd_3$ and Al_2Nd particles distributed in the as-extruded alloys.

Fig.8 shows the optical microstructures of ruptured surface areas and the areas far away from the ruptured surface for the extruded sample alloy I and alloy IV at RT. As seen from Fig.8a, the grains near fracture are stretched along the tensile direction. Extensive deformation twins exist in this area. Some secondary microcracks are located at grain boundaries in alloy IV, as shown in Fig.8c. And similarly, deformation twinning is also observed inside the grains, but less than that in alloy I. While for the microstructure far away from the fracture shown in Fig.8b and 8d, the volume fraction of the twinning is much lower than that near the ruptured surface area.

It is indicated that twins act as complementary deformation mechanism so as to enhance the room temperature ductility. Because of the mismatch between the secondary phase and the matrix, stress concentration easily occurs around

Table 3 Tensile properties of the extruded Mg-Al-Ca-*x*Nd alloys at RT and 150 ℃

Alloy	RT			150 ℃		
	UTS/MPa	YS/MPa	Elongation/%	UTS/MPa	YS/MPa	Elongation/%
I	267	144	20.0	192	140	48.6
II	281	176	19.5	200	145	44.6
III	297	187	18.2	213	151	40.3
IV	304	203	16.9	229	159	39.3

secondary phase particles, finally resulting in the fracture of the alloy. So alloy I and alloy IV exhibit the best and the worst ductility among these four alloys, respectively.

Fig.9 provides SEM fractographs of the fracture surfaces for the tensile specimens of four as-extruded alloys. The fractograph of alloy I shows a ductile fracture mode with a lot of dense and deep dimples, while a few broken particles with a size of several microns can be observed in the fractographs of the Nd added alloys (arrows in Fig.9b~9d). Accordingly, the tensile elongation decreases with Nd content due to the increase of large and fragile particles, and this embedment of coarsening phases induces high stress concentrations with large particles at the particle/matrix interface, which can easily trigger voids to nucleate by particle cracking or particle/matrix interface debonding. This point can be supported by the EDS analysis shown in Fig.10. For the broken polygonal particle under the dimples, EDS result shows that Al:Nd ratio is 2.1:1, close to the ratio 2:1. Based on the XRD results, the polygonal particle can be identified as Al_2Nd phase.

It is also shown that both ultimate tensile strength and yield strength are considerably improved with Nd addition at 150 ℃, but ductility decreases. The poor thermal stability of $Mg_{17}Al_{12}$ phase and its semicontinuous distribution along

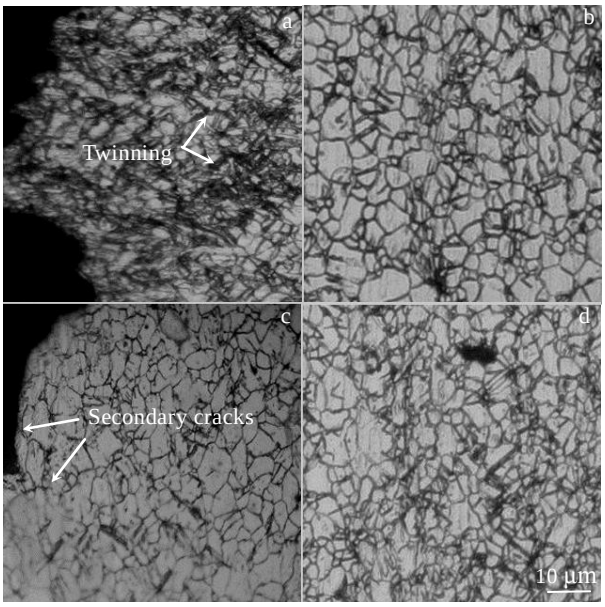

Fig.8 OM images of the fracture surface (a, c) and positions far away from the fracture surface (b, d): (a, b) alloy I and (c, d) alloy IV

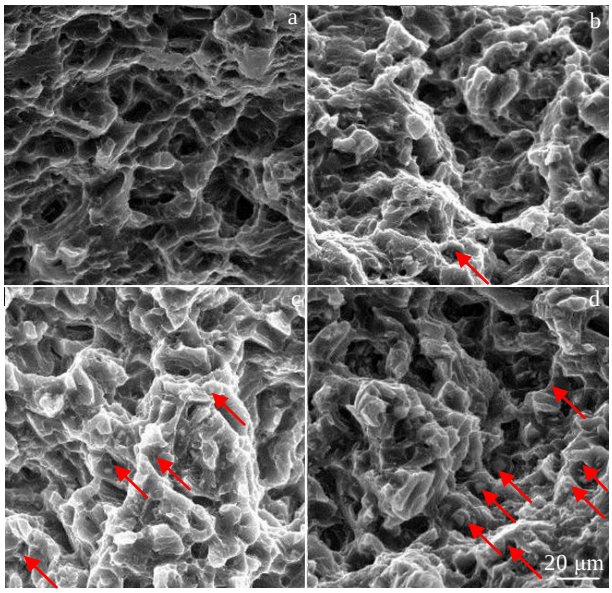

Fig.9 SEM fractographs of fractured tensile samples of extruded Mg-Al-Ca-Nd alloys: (a) alloy I, (b) alloy II, (c) alloy III, and (d) alloy IV

grain boundary contribute to poor creep resistance in alloy I. Due to the formation of relatively thermally stable $Al_{11}Nd_3$ and Al_2Nd precipitates and the complete suppression of $Mg_{17}Al_{12}$ phase with the Nd addition, the strengths of alloy II~IV are improved. But the elongation at 150 ℃ gradually decreases as the amount of Nd addition increases, which is induced by the increase in the amount of Al-Nd particles, and their split effect on the matrix causes the initiation or propagation of cracks.

Table 4 shows the comparative mechanical properties of the previously reported wrought Mg-Al-Nd alloys [20, 22, 29, 30]. The extruded alloy IV in this study has significantly higher mechanical properties than an ECAPed Mg-15Al-1.5Nd alloy and as-cast Mg-Al-Nd-Mn alloy with similar composition, whereas the elongation in this work is lower than the reported elongation of an extruded Mg-Al-Nd-Mn alloy because the latter alloy contains a wide distribution of the Schmid factor[22].

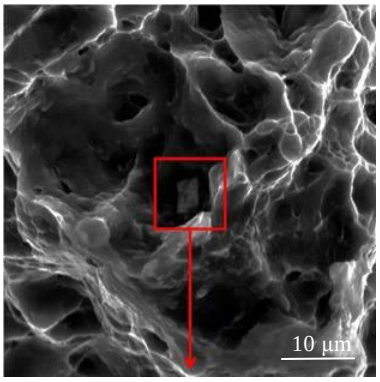

Element	wt%	at%
Mg K	19.87	39.76
Al K	22.68	40.87
Nd K	57.45	19.37
Total	100.00	100.00

Fig.10 Highly magnified SEM micrographs of fractured tensile samples of alloy IV and corresponding EDS results

Table 4 Comparative tensile properties and process condition of Mg alloys with similar composition at high temperature

Composition/wt%	State	UTS/ MPa	TYS/ MPa	Elongation/ %	Ref.
Mg-4Al-0.4Mn-4Nd	Die-cast	140	122	31.0	20
Mg-5Al-2Nd-0.2Mn	Extruded	136	80	62.0	22
Mg-15Al-1.5Nd	ECAPed	186	148	39.6	29
Mg-5Al-2Nd-0.4Mn	Cast	199	79	23.0	30

3 Conclusions

1) There are α-Mg, $Mg_{17}Al_{12}$ and Al_2Ca phases in the Nd-free alloys. When Nd is added, new phases of $Al_{11}Nd_3$ and Al_2Nd can be observed. With increasing the Nd addition, the grain size decreases. The grain sizes of Mg-Al-Ca-*x*Nd (*x*=0, 0.62, 1.11, 1.76, wt%) are 4.80, 4.13, 2.70 and 2.39 μm, respectively.

2) With increment of Nd, the tensile strength increases from 267 MPa to 304 MPa, the yield strength increases from 144 MPa to 203 MPa and the elongation decreases from 20.0% to 16.9% at room temperature in Mg-Al-Ca-*x*Nd alloys. At 150 ℃, the tensile strength increases from 192 MPa to 229 MPa, the yield strength increases from 140 MPa to 159 MPa and the elongation decreases from 48.6% to 29.3% with increasing the Nd content.

3) The increase in tensile strength and yield strength of extruded alloy is attributed to the finer grain size, fragments of Al-Nd secondary phase particles and solid solute strengthening. However, a higher addition of Nd may substantially deteriorate the ductility performance of the alloy.

References

1 Wang X J, Xu D K, Wu R Z *et al*. *Journal of Materials Science and Technology*[J], 2018, 34: 245
2 You S H, Huang Y D, Kainer K U *et al*. *Journal of Magnesium Alloys*[J], 2017, 5: 239
3 Liu H, Huang H, Yang X W *et al*. *Journal of Magnesium Alloys*[J], 2017 5:231
4 Pan F S, Yang M B, Chen X H, *Journal of Materials Science and Technology*[J], 2016, 32: 1211
5 Ding H, Liu L, Kamado S *et al*. *Journal of Alloys and Compounds*[J], 2008, 456: 400
6 Chen X H, Pan F S, Mao J J *et al*. *Materials & Design*[J], 2011, 32: 1526
7 Suhb C, Shim M S, Kim D W *et al*. *Scripta Materialia*[J], 2013, 6: 465
8 Zhang R Q, Wang J F, Huang S *et al. Journal of Magnesium Alloys*[J], 2017, 5: 355
9 Gao S Y, Chen X H, Pan F S *et al*. *Scientific Reports*[J], 2018, 8: 491
10 Zhao C Y, Chen X H, Pan F S *et al*. *Material Science and Engineer A*[J], 2018, 713: 244
11 Moon B G, You B S, Hahn Y D. *Current Nanoscience*[J], 2014, 10: 108
12 Pan F S, Chen X H, Yan T *et al*. *Journal of Magnesium Alloys*[J], 2016, 4: 8
13 Chen X H, Liu J, Pan F S. *Journal of Physics and Chemistry of Solids*[J], 2013, 74: 872
14 Monfared A, Ghaee A, Ebrahimi-Barough S. *Journal of Non-Crystalline Solids*[J], 2018, 489: 71
15 Fu Y, Cao Q P, Liu S Y *et al*. *Scripta Materialia*[J], 2018, 149: 139

16 Liu J, Fu Y, Tang Y *et al*. *Journal of Alloys and Compounds*[J], 2018, 742: 524
17 Kang Q, Jiang H T, Zhang Y *et al*. *Journal of Alloys and Compounds*[J], 2018, 742: 1019
18 Wang J, Liu R D, Dong X G *et al*. *Journal of Rare Earths*[J], 2013, 31: 616
19 Solomon Ellen L S, Marquis Emmanuelle A. *Materials Letter*[J], 2018, 216: 67
20 Zhang J H, Wang J, Qiu X *et al*. *Journal of Alloys and Compounds*[J], 2008, 464: 556
21 Wang J, Fu J W, Dong X G et al. *Materials & Design*[J], 2012, 36: 432
22 Wang J L, Guo Y C, Li J P *et al*. *Journal of Alloys and Compounds*[J], 2015, 653: 100
23 Zhang S C, Wei B K, Cai Q Z *et al*. *Transactions of Nonferrous Metals Society of China*[J], 2003(1): 83
24 Liu H M, Chen Y G, Tang Y B *et al*. *Material Science and Engineer A*[J], 2006, 437: 348
25 Yu Y N. *The Science and Design of Engineering Materials*[M]. Beijing: China Machine Press, 2003: 632 (in Chinese)
26 Kim S H, Kim D H, Kim N J. *Material Science and Engineer A*[J], 1997, 226-228: 1030
27 Liu L Z, Chen X H, Pan F S *et al*. *Material Science and Engineer A*[J], 2015, 644: 247
28 Xu X Y, Chen X H, Du W W *et al*. *Journal of Magnesium Alloys*[J] 2017, 33: 926
29 Cheng W L, Wang W W, Wang H X *et al*. *Material Science and Engineer A* [J], 2015, 633: 63
30 Wang J L, Yang J, Wu Y M *et al*. *Material Science and Engineer A*[J], 2008, 472: 332
31 Zhu T L, Cui C L, Zhang T L *et al*. *Materials & Design*[J], 2014, 57: 245
32 Zhu T L, Sun J F, Cui C L *et al*. *Material Science and Engineer A*[J], 2014, 600: 1
33 Wu R, Yan Y, Wang G *et al*. *International Materials Reviews*[J], 2015, 60(2): 65

Nd 对 Mg-Al-Ca 合金微结构及力学性能影响的研究

杨东虎[1]，陈先华[2,3]，徐笑阳[2]，赵超越[2,3]

(1. 北京理工大学，北京 100081)

(2. 重庆大学 材料科学与工程学院，重庆 400044)

(3. 重庆大学 国家镁合金材料国家工程技术研究中心，重庆 400044)

摘 要：用 OM，SEM 和 XRD 等方法研究了挤压态 Mg-Al-Ca-*x*Nd（*x*=0~1.76，质量分数, %）合金的显微组织和析出相以及该合金在室温和高温下的力学性能。结果表明，Nd 的添加会使基体中形成 Al_2Nd 和 $Al_{11}Nd_3$ 相，并且细化 Mg-Al-Ca 合金的晶粒。随着 Nd 添加量的增加，Al_2Nd 和 $Al_{11}Nd_3$ 相的数量也随之增加。当添加 1.76%Nd 时，合金的平均晶粒尺寸从不含 Nd 的 4.80 μm 变为 2.39 μm。由于第二相的析出和晶粒细化，室温下的力学性能也得到改善。随着 Nd 元素含量的增加，合金的室温抗拉伸强度由 267 MPa 提高到 304 MPa，屈服强度从 144 MPa 提高到 203 MPa，延伸率从 20.0%下降到 16.9%。在 150 ℃时，随着 Nd 含量的增加，拉伸强度从 192 MPa 增加到 229 MPa，屈服强度从 140 MPa 增加到 159 MPa，伸长率从 48.6%下降到 29.3%。

关键词：Mg-Al-Ca-Nd合金；挤压态；微结构；力学性能

作者简介：杨东虎，男，1978 年生，博士，北京理工大学材料学院，北京 100081，电话：010-68945793，E-mail: 171200626@qq.com